Effects of process parameters on the evaporative pattern casting of scrap aluminum–RHA composites

Rudi Siswanto[1*], Abdul Ghofur[1], Rachmat Subagyo[1], Mastiadi Tamjidillah[1], Mahmud[2], Ma'ruf[1] and Adi Nordiman[1]

[1] Department of Mechanical Engineering, Faculty of Engineering, Universitas Lambung Mangkurat, **Indonesia**
[2] Department of Environmental Engineering, Faculty of Engineering, Universitas Lambung Mangkurat, **Indonesia**

*Corresponding Author: rudisiswanto@ulm.ac.id
Received: 16 September 2025; *Revised:* 06 February 2026; *Accepted:* 10 February 2026

Cite this https://doi.org/10.24036/teknomekanik.v9i1.46072

Abstract: This study investigates the fabrication and characterization of aluminium matrix composites reinforced with rice husk ash (RHA), using scrap aluminium as the base material and evaporative pattern casting as the manufacturing method. The work evaluates the effects of three key independent variables: pouring temperature, aluminium (Al)-RHA composition ratios, and styrofoam pattern thickness on the resulting composite properties. The dependent variables examined include surface roughness, Brinell hardness, and dimensional shrinkage-expansion. Experimental results show that increasing the pouring temperature and adjusting the composition ratio significantly influence the mechanical and physical properties of the composites. The highest hardness (45.6 HB) and fluidity (252.65 mm) were achieved at a 60:40 composition ratio and a pouring temperature of 750 °C, albeit at the cost of increased porosity. Additionally, the styrofoam pattern thickness was found to affect the dimensional stability and surface roughness of the composites, with thicker patterns resulting in higher surface roughness. This study highlights the potential of utilizing rice husk ash as a reinforcing material in aluminium matrix composites, offering a sustainable approach to improving material properties. The findings suggest that an optimal balance of composition ratio, pouring temperature, and pattern thickness is crucial to achieving desirable mechanical and physical characteristics, with implications for advanced manufacturing processes in the materials industry.

Keywords: evaporative casting; Al-RHA composite; pouring temperature; pattern thickness, physical-mechanical properties

1. Introduction

The global demand for lightweight, high-performance, and environmentally friendly engineering materials continues to grow as the automotive, agricultural, aerospace, and modern transportation industries develop. One of the most promising solutions is the use of metal matrix composites (MMCs) [1]. Metal matrix composites (MMCs), particularly those based on aluminum, offer excellent mechanical properties, corrosion resistance, and an outstanding strength-to-weight ratio [2], [3]. Aluminum has long been the preferred choice due to its ease of processing and versatile functional characteristics. However, to further enhance this material's performance, reinforcement additives are required. An important approach involves using agro-industrial waste, particularly rice husk ash (RHA). RHA is a promising reinforcement material because it contains high silica content, is economical, widely available, and environmentally friendly, making it an attractive candidate for strengthening aluminium-based composites [3], [4], [5].

It has been demonstrated that incorporating rice husk ash (RHA) at concentrations between 5% and 20% significantly enhances the mechanical properties of aluminum alloys [5]. The importance of effective mixing techniques to ensure a uniform distribution of RHA within the aluminum matrix has also been emphasized [6], as homogeneous dispersion is crucial for achieving improved composite performance. Increased RHA content has been associated with enhanced wear resistance, indicating that RHA-reinforced composites outperform conventional aluminum matrices [5]. However, it has also been cautioned that exceeding the optimal RHA content may increase porosity, which can adversely affect the material's mechanical integrity. Similarly, improvements in the wear behavior of aluminum metal matrix composites following RHA addition have been reported [7], highlighting the need to optimize both reinforcement composition and processing parameters to achieve balanced, reliable composite properties.

Most of these studies employed conventional casting techniques, which may limit the applicability of their findings to more sustainable practices involving scrap aluminium. This is particularly relevant because scrap aluminium offers an eco-friendly and cost-effective alternative that supports sustainable manufacturing practices [8]. The application of circular economy principles is increasingly significant in this context. The use of scrap aluminium as the base material, combined with agricultural waste reinforcement such as RHA, not only reduces reliance on primary materials but also provides a sustainable solution in manufacturing processes [9], [10]. This approach not only reduces production costs but also minimizes the ecological impact associated with mining and refining primary aluminium. Furthermore, the use of agricultural waste aligns with the principles of waste minimization and resource efficiency, which are highly important in the contemporary paradigm of sustainable manufacturing [11]. To effectively produce RHA-reinforced aluminium composites, innovative manufacturing technologies are essential. One such method is evaporative pattern casting (EPC), which enables the production of complex geometries without extensive post-processing. In this technique, polystyrene patterns evaporate upon contact with molten metal, forming precise mold cavities [1], [4], [12]. Reinforcing scrap aluminium with rice husk ash (RHA) using EPC offers promising opportunities to enhance mechanical properties and optimize performance characteristics.

The advantages of EPC compared with traditional casting methods are significant, including improved shape precision, lower energy consumption, and reduced surface defects, provided that process parameters are carefully controlled. However, the application of EPC in aluminium composites, particularly scrap aluminium reinforced with RHA, has not been extensively studied. Most research has focused on techniques such as stir casting and powder metallurgy using pure aluminium as the matrix [13], [14]. The development of scrap aluminium-based composites reinforced with RHA is a highly interesting topic that involves technological, economic, and environmental considerations. By continuing to explore new fabrication techniques such as EPC, extensive research can contribute to optimizing the mechanical properties and manufacturing efficiency of these innovative materials, ensuring their feasibility for advanced engineering applications [15]. Therefore, comprehensive research is needed to investigate key process parameters in EPC, including pouring temperature, pattern thickness, and RHA reinforcement ratio. Such studies should explicitly address their effects on the final composite properties, including density, surface roughness, hardness, porosity, and fluidity length, as these variables strongly influence the performance of the developed materials [4], [14].

The combination of aluminium with RHA produces composites with improved surface characteristics. Uniform distribution of RHA particles within the aluminium matrix helps achieve desirable surface properties [16], [17]. RHA-reinforced composites can reach hardness levels as high as 75.94 HV, which is significantly superior to pure aluminium [18], [17], [19]. This increase in hardness is mainly due to the high silica content of RHA, which contributes to reinforcement mechanisms within the aluminium matrix [18]. When properly integrated into aluminium, RHA

can also produce balanced porosity that optimizes both weight and strength [14]. The presence of RHA improves the flow characteristics of molten aluminium, which are particularly beneficial during the casting process. Improved fluidity can result in higher-quality castings, reduced defects, and enhanced overall performance of the final product [16], [17], [19].

Rice husk ash serves as an effective reinforcement material in scrap aluminium composites produced via evaporative pattern casting, resulting in measurable improvements in surface roughness, hardness, porosity control, and fluidity length. These advantages highlight its effectiveness as a low-cost, environmentally friendly alternative reinforcement. Most previous studies on Al–RHA metal matrix composites have primarily used primary aluminium and conventional fabrication methods, such as stir casting or powder metallurgy. In contrast, this study is distinguished by focusing on scrap aluminium reinforced with RHA produced via evaporative pattern casting (EPC), in which the polystyrene pattern evaporates during filling, making the final quality highly sensitive to pouring temperature, pattern thickness, and the RHA fraction. Therefore, the novelty of this study lies in the systematic quantification of the combined effects of pouring temperature, pattern thickness, and RHA ratio on surface roughness, hardness, porosity, and fluidity length.

2. Material and methods

2.1 Material

In this study, scrap aluminium was obtained from discarded low-voltage (0.6/1 kV) aerial bundled cables (ABC) used in industrial power distribution systems. The chemical composition of scrap aluminium from electrical cables, as tested using Energy Dispersive X-ray Spectroscopy (EDX), is presented in Table 1 and Figure 1, while the physical form of the scrap aluminium is shown in Figure 2.

Table 1. EDX analysis of scrap aluminum from electrical cables

Element	Weigth (%)	Atomic (%)
O K	14.6	22.7
Al K	82.9	76.3
Fe K	2.5	1.1

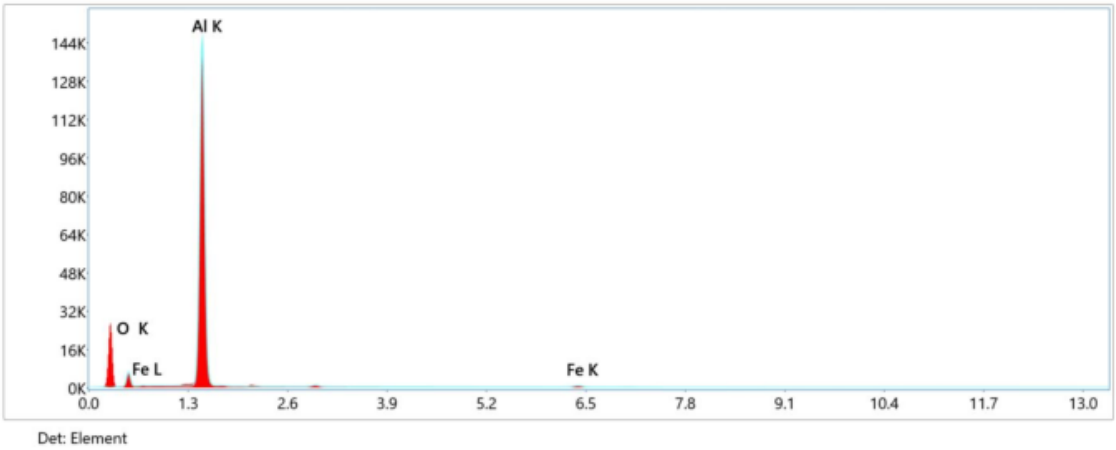

Figure 1. EDX analysis graph of scrap aluminium from electrical cables

Scrap aluminium in storage was found in various forms, including rods, coils, and cut pieces. For melting, the scrap aluminium was cut into 20 cm lengths, as illustrated in Figure 2.

(a) (b)

Figure 2. Scrap aluminium from electrical cables: (a) electrical cable before cutting and (b) aluminium cable cut into 20 cm pieces

The reinforcement material was rice husk ash (RHA), produced through controlled combustion of rice husks in two stages. Stage 1: Combustion in open air at approximately 400 °C for ±3.5 hours. The combustion temperature was measured using a Benetech GM1850 infrared thermocouple with a temperature range of 200–1850 °C. This process produced ash that was mostly black with some white portions. The darker ash contained organic matter and carbon residues [1]. The ash was then ground to a fine powder and sieved through a 200-mesh sieve. Stage 2: Combustion in a furnace at 900 °C for 2 hours using a B-ONE BFNC-2012 furnace with a temperature range of 300–1200 °C. This process produced lighter (white) ash due to the complete combustion of carbon and organic matter. Combustion at this higher temperature produced ash with a higher silica content. The chemical composition of RHA is presented in Table 2 and Figure 3, while the physical form and ash color are shown in Figure 4.

Table 2. EDX analysis of RHA heated at 900 °C for 2 hours

Element	Weigth (%)	Atomic (%)
O K	63.3	75.6
Mg K	0.4	0.3
Si K	35.0	23.7
K K	1.0	0.5

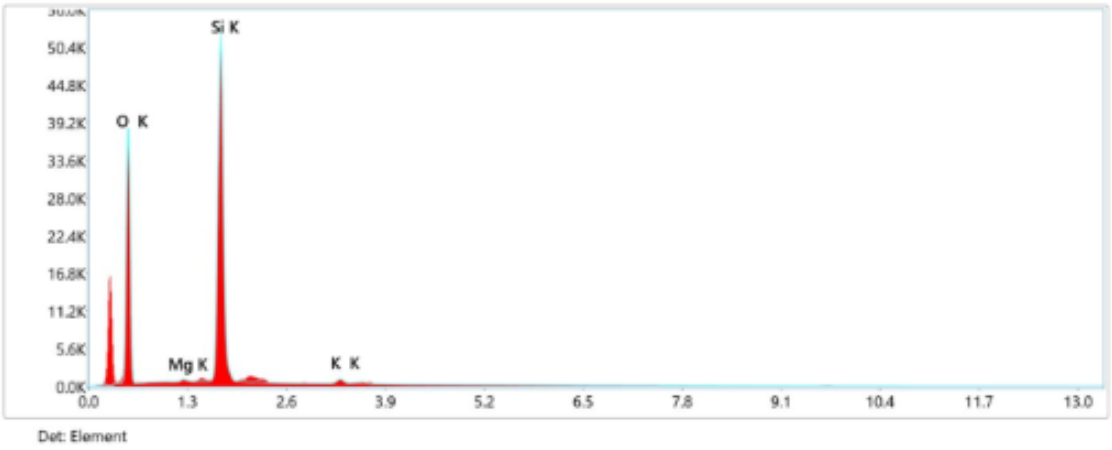

Figure 3. EDX analysis graph of RHA heated at 900 °C for 2 hours

(a) (b) (c)

Figure 4. Rice husk and RHA: (a) raw rice husk, (b) RHA after combustion at 400 °C, and (c) RHA after heating at 900 °C for 2 hours

The styrofoam patterns were obtained from discarded electronic packaging and used as the primary pattern material for specimen fabrication. The waste styrofoam was cut according to the design and assembled with adhesive to form a complete pattern. Variations in pattern thickness were set at 1, 2, 3, 4, 5, 6, and 10 mm, with a width of 10 mm and a length of 400 mm. The visual appearance of the patterns is shown in Figure 5.

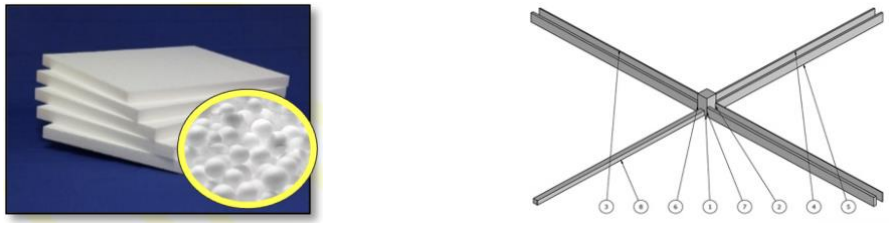

(a) (b)

Figure 5. Styrofoam patterns: (a) raw Styrofoam and (b) shaped pattern

A mold frame was constructed from plywood to hold and stabilize the styrofoam pattern during the casting process (Figure 6).

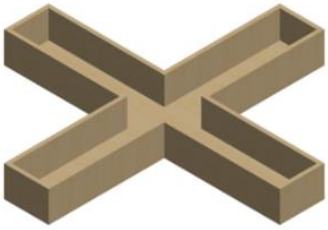

Figure 6. Mold frame

The moulding sand used was local silica sand (Palangka sand). The silica sand was sieved to obtain fractions passing through a 60-mesh sieve. This fine-grained sand was selected due to its permeability and stability, ensuring accurate reproduction of pattern details during casting. The chemical composition of silica sand is shown in Table 3 and Figure 7.

Table 3. EDX analysis of silica sand

Element	Weigth (%)	Atomic (%)
O K	61.6	73.8
Si K	38.4	26.2

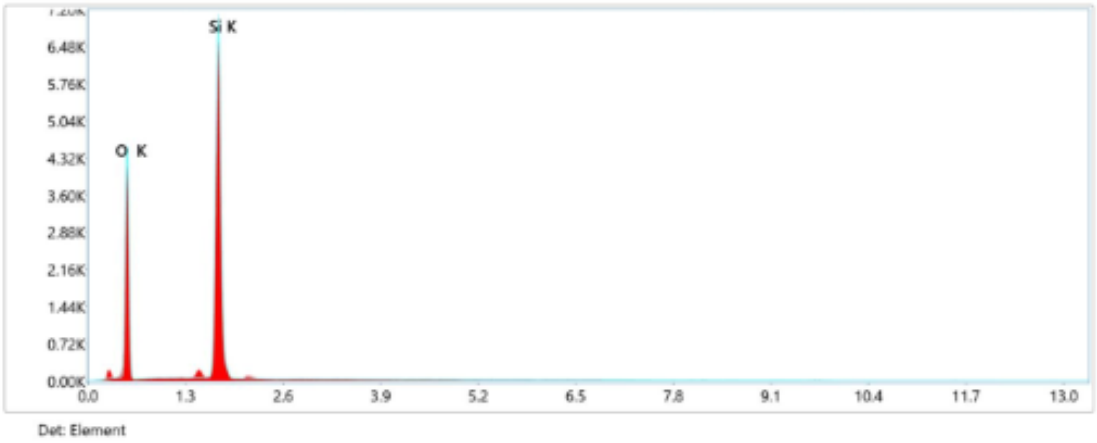

Figure 7. EDX analysis graph of silica sand

The silica sand particles were fine, uniform, and evenly distributed, with a bright white and glossy appearance. They were hard in nature and chemically inert, showing no reactivity with most substances. The morphology and color of the silica sand are shown in Figure 8.

Figure 8. Silica sand (Palangka sand)

2.2 Production of Al-RHA composites

The fabrication of Al-RHA composites was carried out using the evaporative pattern casting method. At the initial stage, styrofoam patterns with various thicknesses were prepared and embedded in dry silica sand within the mold frame. The Al-RHA mixture was formulated in three weight ratios: 70:30, 65:35, and 60:40 between aluminium (Al) and rice husk ash (RHA). Although several Al–RHA MMC studies fabricated by conventional routes report deteriorated properties above ~20 wt.% reinforcement due to porosity and agglomeration, the present work intentionally investigated a higher RHA window (30–40 wt.%) to characterize the upper-loading regime under evaporative pattern casting. This range was selected to quantify process-specific trade-offs among hardness improvement, gas-related porosity, and melt flow (fluidity) behavior in scrap Al-based EPC systems.

Scrap aluminium was melted in a crucible furnace until liquefied, after which RHA was gradually added into the melt. During mixing, the molten metal was continuously stirred at 150 rpm for two minutes to ensure a homogeneous distribution of RHA particles within the aluminium matrix. Subsequently, the molten Al-RHA mixture was poured into the mold containing the styrofoam pattern. This pouring process produced castings as the molten metal filled the mold cavity while vaporizing the styrofoam (Figure 9).

The castings were allowed to solidify in the mold for 30 minutes before being removed, cleaned, and cut into test specimens. Several properties were analyzed, including surface roughness, Brinell hardness (HB), porosity, and fluidity length. Surface roughness was measured using a profilometer, hardness was tested using a Brinell Hardness Tester, porosity was evaluated through the wet–dry

mass difference method and calculated as a percentage, while fluidity length was determined based on the distance that molten metal was able to fill in the mold cavity before solidification occurred.

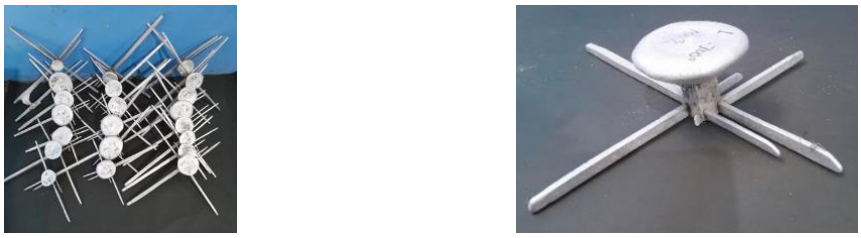

(a) (b)

Figure 9. Al-RHA composites produced by evaporative pattern casting: (a) triplicate samples, (b) sample (perspective view)

2.3 Experimental design

This study employed a factorial design, which enables a comprehensive analysis of the effects of each variable and its interactions. Three independent variables were defined in the experiment: pouring temperature (650 °C, 700 °C, and 750 °C), Al-RHA scrap composition ratios (70:30%, 65:35%, and 60:40%), and styrofoam pattern thickness (1, 2, 3, 4, 5, 6, and 10 mm). The selected ranges were intended to thoroughly evaluate the influence of key parameters in the evaporative pattern casting process on the quality of the resulting composites. The dependent variables observed included surface roughness (μm), Brinell hardness (HB), porosity (%), and fluidity length (mm). Surface roughness was used to assess the quality of the castings, while Brinell hardness indicated the material's mechanical strength. Porosity was measured to evaluate the density and homogeneity of the internal structure, whereas fluidity length was defined as an indicator of the molten metal's ability to fill mold cavities. These four parameters were chosen because they represent the main physical and mechanical characteristics that determine the performance of Al-RHA composites.

2.4 Testing and characterization

Characterization was carried out to evaluate the physical and mechanical properties of the Al-RHA composites. Surface roughness was measured using a surface profilometer, which provided quantitative data on the smoothness and surface quality of the casting. This parameter is important because it affects the product's functional and aesthetic properties and determines the suitability of the specimens for further applications. The surface roughness test was conducted in accordance with ASTM D441 Method C, using a Krisbow KW 06-303 surface roughness tester. Brinell hardness testing was performed in accordance with ASTM E110, using a steel ball indenter under a specified load. The Brinell hardness (HB) values obtained indicated the material's resistance to plastic deformation and served as a key indicator of the composite's mechanical performance. Hardness tests were conducted using a MITECH MH600 hardness tester.

Porosity was determined using the mass volume method by comparing the theoretical and actual densities of the samples. The porosity level is directly related to the strength, wear resistance, and load-bearing capacity of the composites. Generally, higher porosity corresponds to lower mechanical performance. The percentage value of AMMC composite porosity was determined by pycnometric testing in accordance with ASTM B962. Fluidity length was evaluated using a standard Qudong fluidity test mold by measuring the maximum distance that molten metal could flow before solidification. This method has the advantage of providing uniform distribution of molten metal flow across eight channels, as the central gating system is positioned at the middle of the mold [4]. Fluidity length was measured using a caliper from the gating point to the maximum length of the

fully formed casting. This parameter indicates the molten metal's ability to fill the mold cavity, which directly affects the quality of defect-free castings. All test data were systematically recorded and analyzed to identify the effects of process variables, including pouring temperature, Al-RHA composition, and pattern thickness on the measured properties. This analysis aimed to establish clear relationships between evaporative pattern casting process parameters and the performance of the resulting Al-RHA composites.

3. Results and discussion

3.1 Microstructure

Figure 10 presents the photo results of the microstructure of Aluminum (Al) composite reinforced with Rice Husk Ash (RHA) produced through evaporative casting at a pouring temperature of 750 °C with a magnification of 365x.

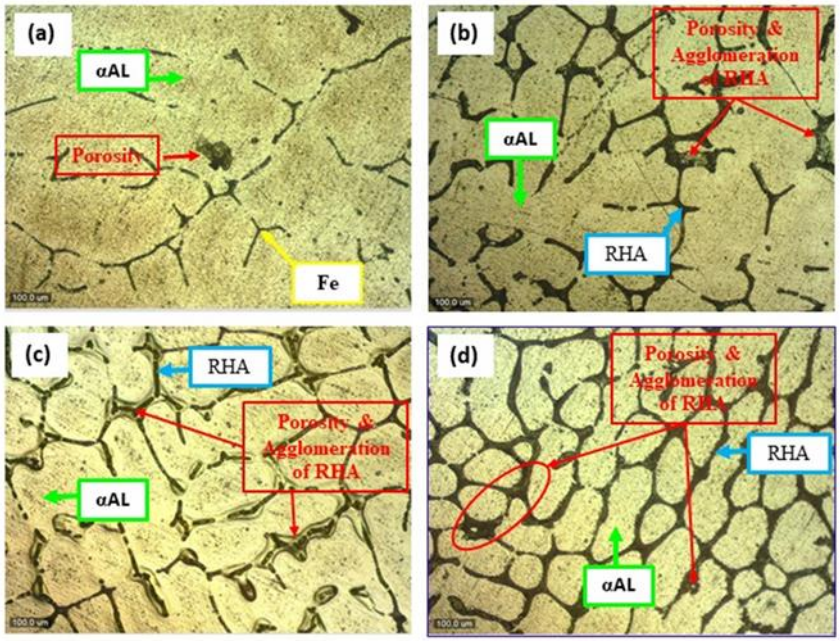

Figure 10. Microstructural photographs of the Al–RHA composite, with compositions: (a) 100–0%, (b) 70–30%, (c) 65–35%, (d) 60–40%

Figure 10(a) shows the microstructure of pure Aluminum (αAl) without RHA reinforcement. The structure appears to have fine grains distributed homogeneously, with minimal porosity. The homogeneity of the grains contributes to the improvement of the material's mechanical properties, as the grain boundaries act as barriers to dislocation movement, thereby enhancing both strength and ductility [5], [20], [21]. Figure 10(b) presents the microstructure of a composite with an Al-RHA (70:30)% composition. The formation of porosity and RHA deposition within the structure is evident. The influence of RHA becomes more apparent as porosity increases and RHA agglomerations grow larger. The addition of RHA into the Al matrix results in a more heterogeneous distribution, where RHA particles potentially disrupt the arrangement of Al grains and form RHA particle aggregates, causing an increase in porosity within the structure [22]. Figure 10(c) shows the microstructure of a composite with an Al-RHA (65:35)% composition. The interaction between the Al matrix and RHA particles is more clearly visible. RHA agglomeration becomes more pronounced, and porosity increases further compared to the previous composition. The interaction between RHA particles and aluminium leads to a more heterogeneous structure, with more noticeable agglomeration and distribution of RHA particles within the Al matrix [22]. Figure 10(d) shows the microstructure of a composite with an Al-RHA (60:40)% composition. At

this composition, the influence of RHA becomes more dominant. The microstructure reveals that RHA particles are more widely distributed within the Al matrix, with increasingly noticeable RHA agglomerations. The increased RHA content results in a significant increase in porosity and the formation of more RHA clusters within the structure. This increase in porosity is related to the uneven distribution of RHA particles in the Al matrix [22].

3.2 SEM analysis

Figure 11 shows SEM test results of an aluminium (Al) composite reinforced with rice husk ash (RHA) produced by evaporative casting at a pouring temperature of 750°C at 1000x magnification.

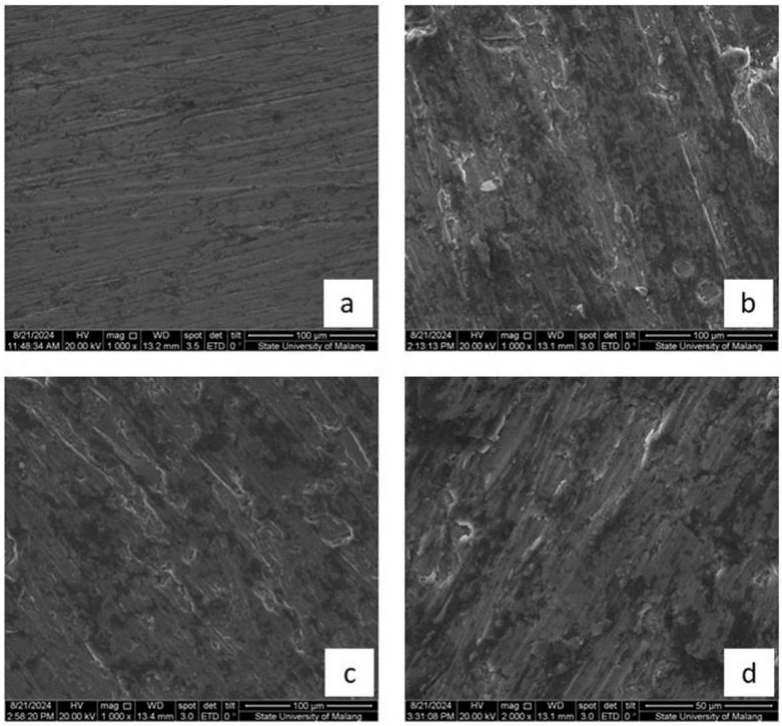

Figure 11. SEM photographs of Al-RHA (%) composites; (a) 100-0, (b) 70-30, (c) 65-35, (d) 60-40

SEM analysis of the fracture surfaces was conducted at a magnification of 1000× to evaluate reinforcement dispersion, agglomeration behavior, porosity characteristics, and particle matrix interfacial integrity. The fracture surface of aluminium without RHA addition (100:0) exhibits a smooth, homogeneous, and continuous morphology accompanied by pronounced plastic deformation features. This behavior is attributed to the inherent ductility of aluminium, which allows significant plastic deformation under applied stress [5], [23]. These characteristics indicate a ductile fracture mechanism dominated by the α-Al matrix. Moreover, no interfacial discontinuities or porosity are observed, confirming a relatively uniform stress distribution within the matrix.

At the Al–RHA composition of 70:30, the fracture surface begins to show localized roughening and the emergence of micro-voids, indicating the early stages of interfacial debonding between RHA particles and the aluminium matrix. With increasing RHA content, the fracture surface becomes progressively rougher, accompanied by a higher density of micro-voids, reflecting intensified interfacial debonding. At higher reinforcement levels (65:35 and 60:40), pronounced RHA agglomeration, particle pull-out features, and irregular porosity are clearly observed. These features signify weak particle matrix interfacial bonding, where agglomerated regions act as stress concentrators that facilitate crack initiation, increase gas entrapment, and promote enhanced porosity formation during the evaporative casting process.

In particular, the presence of larger voids and more frequent agglomeration at higher RHA contents contributes to increased brittleness and reduced ductility of the composites [5], [24]. Such porosity adversely affects tensile strength and ductility by serving as preferential sites for stress concentration and crack propagation [24], [25]. Furthermore, particle agglomeration is commonly associated with poor reinforcement dispersion and inadequate interfacial adhesion, leading to regions with elevated porosity that significantly compromise the mechanical integrity of the composite material [5], [9], [23], [26].

3.3 Surface roughness

Figure 12 presents the surface roughness of aluminum (Al)–RHA composites at different composition ratios (70:30%, 65:35%, 60:40%) and pouring temperatures (650 °C, 700 °C, 750 °C). Based on the data in Figure 12, an analysis was conducted to examine the effects of pouring temperature and Al-RHA composition on composite surface roughness.

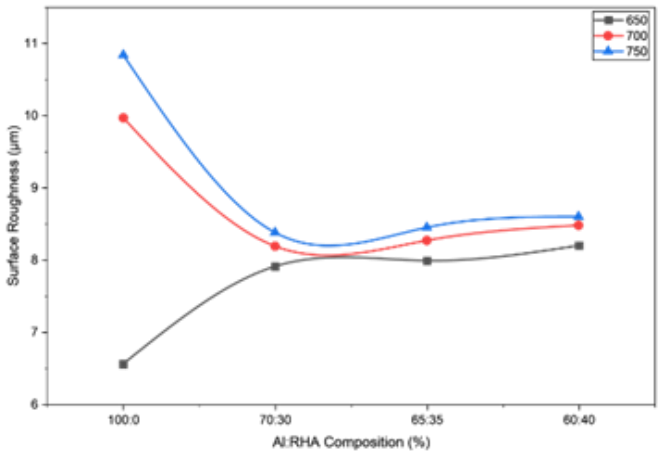

Figure 12. Surface roughness graph of Al-RHA composites

In the aluminium-rice husk ash (RHA) composites manufactured using evaporative pattern casting, surface roughness was observed to increase slightly with both higher pouring temperature and greater RHA proportion. This finding is consistent with previous studies [4], which reported that higher pouring temperatures lead to increased surface roughness. Specifically, at constant composition, raising the temperature from 650 °C to 750 °C resulted in surface roughness values ranging from 7.91 µm to 8.6 µm. The highest roughness was recorded at the 60:40 Al:RHA ratio at the highest temperature. This behavior is likely influenced by increased turbulence during molten metal flow at elevated temperatures, which enhances interactions between the liquid aluminium matrix and RHA, thereby affecting the final surface finish [27]. Previous studies also indicated that turbulence can cause inconsistent flow patterns, producing rougher surfaces due to changes at the metal–decomposition interface [28].

The Al-RHA composition also played a significant role in determining surface quality. Increasing the RHA fraction from 30% to 40% raised the surface roughness of the composites, with the highest Ra value recorded at the Al:RHA (60:40) composition poured at 750 °C (8.6 µm). This suggests that the addition of RHA, which is rich in SiO_2, increases the surface roughness of the composites [4]. Moreover, higher RHA content increases the number of solid particles in the melt. These particles may disrupt uniform flow, resulting in a rougher surface finish and potentially trapping gases from the thermal decomposition of organic matter within the RHA, further influencing surface characteristics. Studies have shown that a higher solid fraction can lead to greater surface roughness, as the particles hinder optimal molten metal flow and solidification, creating more microvoids [5]. The interaction between pouring temperature and Al:RHA composition revealed

that temperature effects were more dominant at lower RHA content (70:30). At this composition, increasing the temperature from 650 °C to 700 °C caused a larger rise in Ra compared with the same temperature increase at higher RHA content (60:40). This indicates that at lower RHA content, higher pouring temperatures lead to more pronounced surface changes, whereas at higher RHA content, temperature increases have a relatively smaller impact on surface roughness.

3.4 Brinell Hardness (HB)

Figure 13 shows the Brinell hardness values of Al-RHA composites at different alloy compositions (70:30%, 65:35%, 60:40%) and pouring temperatures (650 °C, 700 °C, 750 °C). Based on the data in Figure 13, an analysis was conducted to examine the effects of pouring temperature and Al-RHA composition on composite hardness.

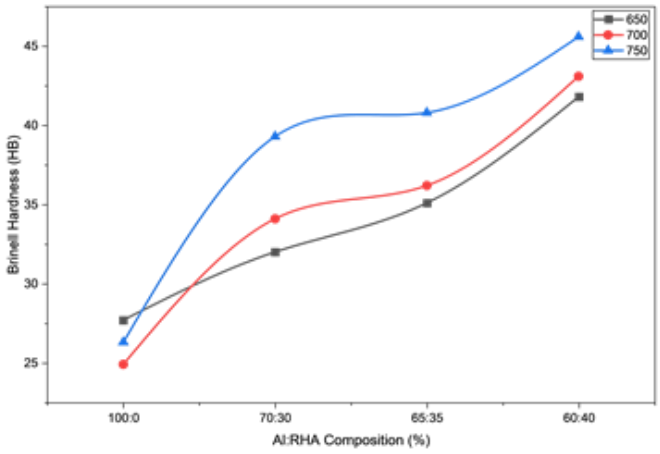

Figure 13. Brinell hardness (HB) graph of Al-RHA composites

The results indicate that Brinell hardness increases with higher pouring temperature. At a composition of 70:30 (Al:RHA), hardness was recorded at 32 HB at 650 °C, rising to 39.3 HB at 750 °C. A similar trend was observed for the 65:35 and 60:40 compositions, with hardness increasing from 35.1 HB (650 °C) to 45.6 HB (750 °C) at the 60:40 composition. Higher temperatures accelerated reactions between Al and RHA particles, improving the dispersion of RHA in the Al matrix and, in turn, enhancing composite hardness.

Brinell hardness also increased with higher RHA fractions in the Al-RHA composition. At 650 °C, hardness rose from 32 HB at 70:30 to 35.1 HB at 65:35, reaching 41.8 HB at 60:40. The most significant increase in hardness occurred with the combined effect of higher RHA content and higher pouring temperature, peaking at 45.6 HB for the 60:40 Al:RHA ratio poured at 750 °C. The same trend was also observed at 700 °C and 750 °C, where the 60:40 composition consistently showed the highest hardness (45.6 HB at 750 °C). This indicates that at higher temperatures, the reinforcing effect of RHA becomes more pronounced, as greater RHA content strengthens the bonding between the metallic matrix and the ceramic reinforcement. These findings are consistent with previous studies, which reported that increasing reinforcement content generally improves the resistance of aluminium matrices to plastic deformation [29]. The improvement in hardness can also be attributed to better matrix–reinforcement bonding at elevated temperatures, which enhances wettability and adhesion between aluminium and RHA particles [5].

Ariff et al. [27] reported that composites reinforced with rice husk ash (RHA) exhibited increased porosity and tensile strength, which was primarily attributed to improved particle distribution within the matrix, resulting in enhanced mechanical performance. These findings are consistent with the observations of [21], [1] who demonstrated significant improvements in key mechanical

properties of aluminium-based composites when RHA was combined with fly ash as a reinforcing material. Similarly, [30] reported that aluminium matrix composites containing RHA showed enhanced tensile strength due to effective stress transfer mechanisms facilitated by the presence of RHA. Furthermore, the incorporation of RHA was found to improve both tensile strength and hardness, an effect associated with the fine particle size and high silica content of RHA, which promotes stronger interfacial bonding within the aluminium matrix [31].

3.5 Porosity

Figure 14 illustrates the porosity of Al-RHA composites at different alloy compositions (70:30%, 65:35%, 60:40%) and pouring temperatures (650 °C, 700 °C, 750 °C). Based on the data in Figure 14, an analysis was conducted to evaluate the effects of pouring temperature and Al-RHA composition on composite porosity.

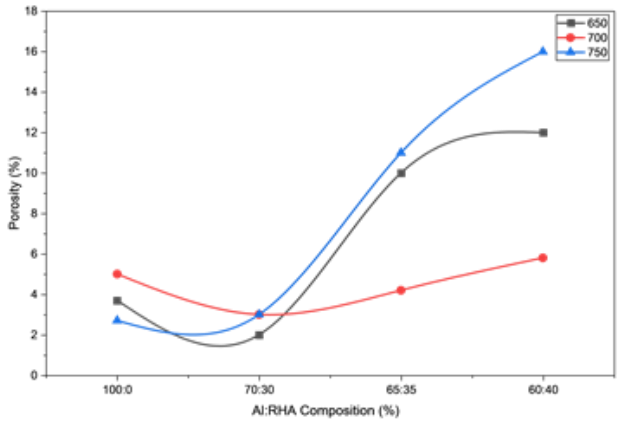

Figure 14. Porosity graph of Al-RHA composites

From Figure 14, it can be seen that the porosity of the composites increased with higher pouring temperatures. At a pouring temperature of 650 °C, the composite with a 70:30 (Al:RHA) composition exhibited a porosity of approximately 5%. However, at a higher pouring temperature of 750 °C, porosity rose sharply to around 10% for the same composition. A similar trend was observed for the 65:35 and 60:40 compositions, where increasing the pouring temperature from 650 °C to 750 °C resulted in greater porosity growth. The increase in porosity at higher temperatures can be explained by the faster burning rate of the styrofoam pattern, which generates a larger volume of gas. These gases are not fully expelled during pouring, leading to voids or pores in the composite. In addition, higher temperatures improve the fluidity of the molten metal, allowing it to flow more rapidly into the mold, but also raising the likelihood of void or pore formation inside the composite. Therefore, higher pouring temperatures not only worsen surface quality but also increase the composite's porosity. This porosity increase at higher RHA content and elevated temperatures is caused by gas entrapment resulting from both the decomposition of the styrofoam pattern and the organic matter in the RHA. The entrapped gases arise from the breakdown of binders and organic constituents present in the RHA [32]. Excessive reinforcement can also hinder the flow and solidification of molten metal, leading to microvoid formation, a phenomenon consistently observed in aluminium-RHA composites [33].

3.6 Fluidity length

Figure 15 presents the fluidity length of Al-RHA composites at different alloy compositions (70:30%, 65:35%, 60:40%) with pouring temperatures (650 °C, 700 °C, 750 °C) and pattern thicknesses (1, 2, 3, 4, 5, 6, 10 mm). Based on the data in Figure 15, an analysis was conducted to

examine the effects of pouring temperature and Al-RHA composition on the achievable fluidity length of the composites.

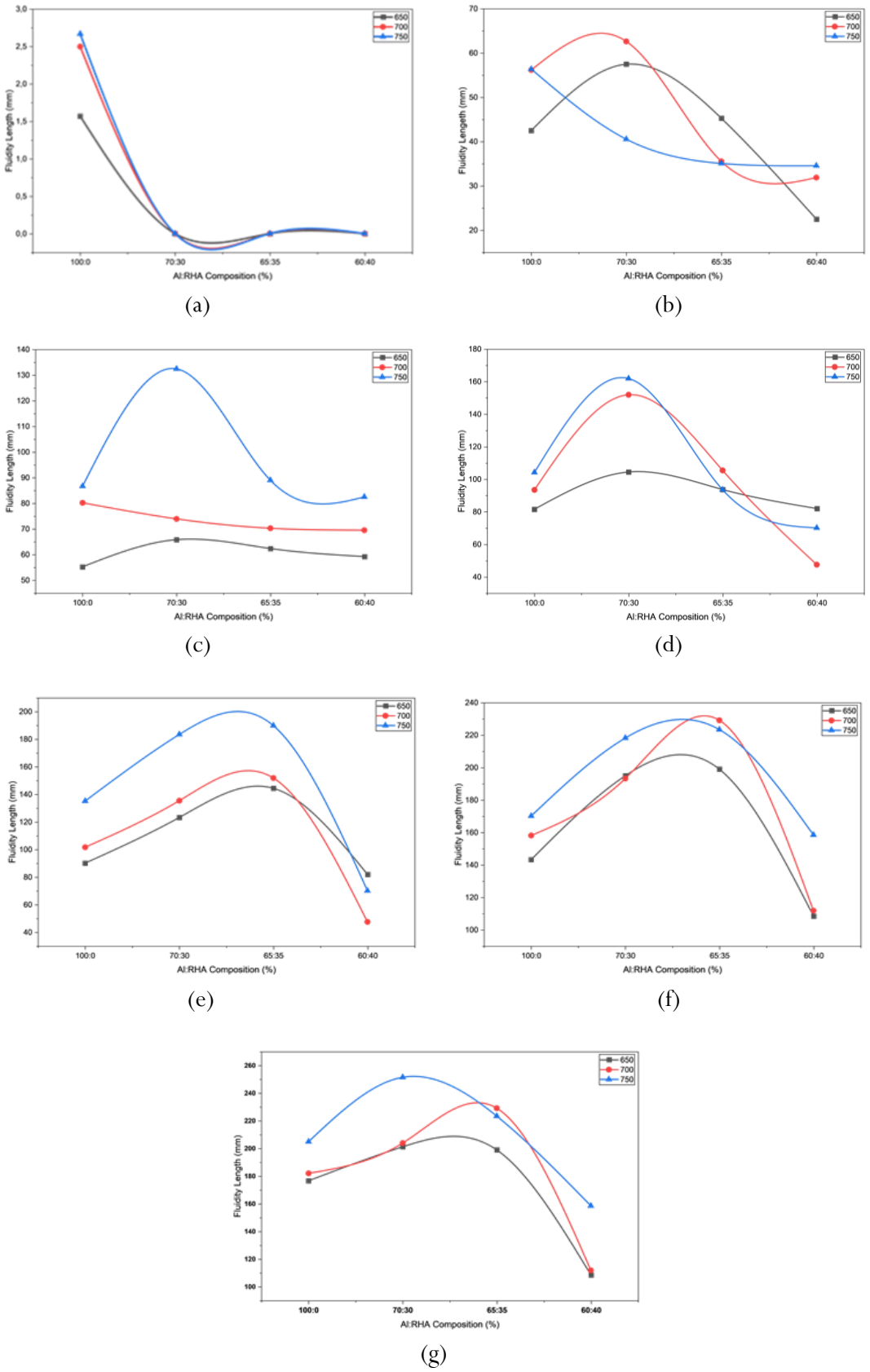

Figure 15. Fluidity length graph of Al-RHA composites; (a) pattern thickness 1 mm, (b) pattern thickness 2 mm, (c) pattern thickness 3 mm, (d) pattern thickness 4 mm, (e) pattern thickness 5 mm, (f) pattern thickness 6 mm, and (g) pattern thickness 10 mm

Fluidity length increased consistently with higher pouring temperatures, particularly at lower RHA contents. At an Al:RHA ratio of 70:30 and a pouring temperature of 750 °C, fluidity reached 251.62 mm. However, at higher RHA content (60:40), fluidity was lower, especially at lower pouring temperatures. The increase in fluidity at elevated temperatures is attributed to the reduced viscosity of the melt and the higher momentum of the molten metal. Conversely, the decrease in fluidity with increasing RHA content is likely due to greater melt resistance and particle interference during flow. The relationships among fluidity length, pattern thickness, pouring temperature, and Al:RHA composition are crucial for understanding and optimizing molten metal flow behavior during casting. Fluidity length is a key parameter as it determines how far molten metal can travel within the mold before solidifying, which is influenced by factors such as pattern thickness, pouring temperature, and alloy composition.

Pattern thickness was found to affect fluidity length significantly. Thinner patterns (1–2 mm) exhibited shorter fluidity lengths due to increased flow resistance, leading to faster solidification compared with thicker patterns (5–10 mm), which allowed longer flow paths and reduced resistance [34]. Thicker patterns also reduced the effect of rapid heat loss, enabling molten metal to travel further within the mold. Previous studies have shown that flow dynamics in casting are closely related to thermal gradients and the resulting solidification kinetics [35].

Pouring temperature also played an important role in influencing fluidity length. Higher pouring temperatures (e.g., 750 °C) correlated with longer fluidity lengths compared with lower temperatures (e.g., 650 °C), due to increased thermal energy, which enhanced the kinetic energy of molten metal particles, reduced viscosity, and facilitated easier flow [36]. The fluidity of the molten matrix showed a consistent pattern with temperature. It increased with higher temperatures, particularly at lower RHA contents. However, with higher RHA content (60:40), fluidity decreased, likely due to increased melt resistance and disturbances caused by solid particles in the molten flow [37].

The concept of superheat further explains this phenomenon; as pouring temperature increases, it extends the cooling time of the molten metal before solidification, reduces resistance to premature nucleation, and prevents flow disruption [36]. Nonetheless, excessively high temperatures can have counterintuitive effects, especially due to the pyrolytic behavior of EPS patterns, which may generate additional gases that increase back pressure and hinder fluid flow [38]. The interaction between pattern thickness and temperature showed varying effects on fluidity. In thinner patterns, pouring temperature and composition played a more critical role due to rapid solidification rates that limited flow. In thicker patterns, temperature effects were more dominant, as sufficient heat retention allowed better flow even at higher RHA content [36][4]. Thus, the improvement in fluidity length is not solely a function of temperature increase or composition change, but rather requires a careful balance tailored to the specific characteristics of the mold and the molten alloy.

3.7 Statistical test

Statistical analysis was conducted using analysis of variance (ANOVA) to evaluate the effects of composition, pouring temperature, and their interaction on surface roughness, hardness, and porosity. All measurements were conducted in triplicate ($n = 3$). Surface roughness exhibited the lowest variability (SD ≈ 0.47 µm; 95% CI ±0.57 µm), hardness showed moderate variability (SD ≈ 4.23 HB; 95% CI ±5.12 HB), while porosity presented the highest dispersion (SD ≈ 4.48%; 95% CI ±5.43%), reflecting the inherent process variability of evaporative casting.

Statistical evaluation using ANOVA showed that surface roughness was not significantly affected by either composition or pouring temperature ($p > 0.05$), and no interaction effect was observed. Tukey post-hoc tests confirmed the absence of significant differences across all compositional and

temperature levels, indicating stable, reproducible surface formation during evaporative casting. In contrast, hardness was significantly influenced by both composition ($p < 0.01$) and pouring temperature ($p < 0.05$), while their interaction was not significant. Post-hoc analysis revealed that higher reinforcement compositions differed significantly from the lowest, and a significant increase in hardness was observed at the highest pouring temperature.

For porosity, a significant effect of composition was identified ($p < 0.05$), whereas pouring temperature and interaction effects were not statistically significant. Tukey analysis indicated that porosity differences were mainly associated with compositional variation, suggesting that pore formation was predominantly governed by reinforcement content rather than thermal conditions. Overall, the results demonstrate that surface quality is relatively insensitive to processing variations, while hardness and porosity are primarily controlled by composition, with hardness additionally affected by pouring temperature.

An anomalous saturation behavior was observed in surface roughness at higher RHA content (60:40), where further increases in pouring temperature resulted in only marginal changes. This suggests that beyond a critical reinforcement threshold, surface morphology is predominantly governed by particle interference rather than thermal turbulence. In contrast, hardness exhibited a pronounced non-linear response, with a disproportionately large increase at the 60:40 composition when poured at 750 °C, indicating a temperature-activated reinforcement mechanism in which effective load transfer and interfacial bonding occur only above a critical superheat level.

Although porosity visibly increased at elevated temperatures, statistical analysis revealed that temperature was not the dominant controlling factor. Instead, this anomalous behavior indicates that gas evolution associated with RHA and pattern decomposition outweighed thermal effects, leading to composition-controlled and stochastic pore formation. Meanwhile, fluidity length displayed an unexpected behavior at high RHA content (60:40) and 750 °C, where relatively high fluidity was retained despite increased particle loading. This suggests a competing mechanism in which enhanced melt superheat partially compensates for particle-induced flow resistance, particularly when combined with thicker pattern geometries.

4. Conclusion

The study demonstrated that higher pouring temperatures (700–750 °C) and greater RHA content significantly influenced the properties of Al-RHA composites. Surface roughness increased with both temperature and RHA fraction, while hardness improved markedly, reaching a maximum of 45.6 HB at 60:40 composition and 750 °C. Porosity also rose under these conditions due to greater gas entrapment and particle interference. Fluidity length increased with higher temperatures and thicker patterns, but decreased with higher RHA fractions.

Author's declaration

Author contribution

All authors contributed to this paper: **Rudi Siswanto** contributed to the idea, conception, and design of the research, as well as data analysis, and wrote the manuscript (grantee as chair). **Abdul Ghofur** (grantee as member) prepared the materials, analysed the data, and wrote the draft and main manuscript. **Rachmat Subagyo** contributed to data analysis, statistics, and correction of the main journal draft. **Mastiadi Tamjidillah** was responsible for data analysis and discussion. **Mahmud** made corrections and revisions to the manuscript. **Ma'ruf** handled the casting operations, specimen preparation, and data collection. **Adi Nurdiman** carried out the casting

operations, specimen preparation, and data collection. Therefore, all authors contributed to and approved this final manuscript for publication.

Funding statement

This research was funded by a grant from the Lambung Mangkurat University Public Service Agency, Fiscal Year 2025, Number: SP DIPA-139.03.2.693381/2025.

Data Availability

The data for this research are available. If you wish to use them as a basis for your research, please contact the authors.

Acknowledgements

We express our deepest gratitude to the heads of laboratories and technicians in the Manufacturing and Materials Processes Laboratory, Faculty of Engineering, Universitas Lambung Mangkurat.

Competing interest

All authors declare that they have no conflicts of interest related to this research.

Ethical clearance

This research did not involve human or animal as the subjects.

AI statement

This article is the original work of the authors. No AI software was used to write the sentences and/or create/edit the tables and figures in this manuscript.

Publisher's and Journal's note

Universitas Negeri Padang as the publisher, and Editor of Teknomekanik state that there is no conflict of interest towards this article publication.

References

[1] R. Siswanto, R. Subagyo, M. Tamjidillah, Mahmud, and M. S. I. Setiawan, "Identifying the influence of pouring temperature, Al-RHA composition, and pattern thickness on the properties of Al-RHA composites produced by evaporative casting," *Eastern-European Journal of Enterprise Technologies*, vol. 5, no. 12(131), pp. 39–49, 2024, https://doi.org/10.15587/1729-4061.2024.310274

[2] B. Parveez, M. A. Maleque, and N. A. Jamal, "Influence of agro-based reinforcements on the properties of aluminum matrix composites: a systematic review," *Journal of Materials Science*, vol. 56, no. 29. Springer, pp. 16195–16222, Oct. 01, 2021. https://doi.org/10.1007/s10853-021-06305-2

[3] S. P. Dwivedi, P. Sharma, and A. Saxena, "Utilization of waste spent alumina catalyst and agro-waste rice husk ash as reinforcement materials with scrap aluminium alloy wheel matrix," *Proceedings of the Institution of Mechanical Engineers, Part E: Journal of Process Mechanical Engineering*, vol. 234, no. 6, pp. 543–552, Dec. 2020, https://doi.org/10.1177/0954408920930634

[4] R. Siswanto, R. Subagyo, M. Tamjidillah, Mahmud, and S. A. Setiawan, "Utilization of rice husk ash waste and scrap aluminum ascomposite materials fabricated by evaporative casting," *Mechanical Engineering for Society and Industry*, vol. 4, no. 2, pp. 294–307, Dec. 2024, https://doi.org/https://doi:10.31603/mesi.12505

[5] A. Y. Awad, M. N. Ibrahim, and M. K. Hussein, "Effects of Rice Husk Ash–Magnesium Oxide Addition on Wear Behavior of Aluminum Alloy Matrix Hybrid Composites," *Tikrit Journal of Engineering Sciences*, vol. 25, no. 4, pp. 16–23, Dec. 2018, https://doi.org/10.25130/tjes.25.4.04

[6] J. A. K. Gladston, I. Dinaharan, N. M. Sheriff, and J. D. R. Selvam, "Dry sliding wear behavior of AA6061 aluminum alloy composites reinforced rice husk ash particulates produced using compocasting," *Journal of Asian Ceramic Societies*, vol. 5, no. 2, pp. 127–135, Jun. 2017, https://doi.org/10.1016/j.jascer.2017.03.005

[7] S. Mustafa, J. Haider, P. Matteis, and Q. Murtaza, "Synthesis and Wear Behaviour Analysis of SiC- and Rice Husk Ash-Based Aluminium Metal Matrix Composites," *Journal of Composites Science*, vol. 7, no. 9, Sep. 2023, https://doi.org/10.3390/jcs7090394

[8] G. F. Aynalem, "Processing Methods and Mechanical Properties of Aluminium Matrix Composites," *Advances in Materials Science and Engineering*, vol. 2020. Hindawi Limited, 2020. https://doi.org/10.1155/2020/3765791

[9] O. O. Joseph and K. O. Babaremu, "Agricultural waste as a reinforcement particulate for aluminum metal matrix composite (AMMCs): A review," *Fibers*, vol. 7, no. 4. MDPI Multidisciplinary Digital Publishing Institute, Apr. 01, 2019. https://doi.org/10.3390/fib7040033

[10] A. Seshappa, K. Prudhvi Raj, B. Subbaratnam, U. Pranavi, N. srihithagunapriya, and S. Chhabra, "Investigations of Al-Manufacturing while 7075/RHA/Al 2 O 3 Composite by Squeeze Casting Approach"," *MATEC Web of Conferences*, vol. 392, p. 01027, 2024, https://doi.org/10.1051/matecconf/202439201027

[11] R. Senthil and M. Vinayagam, "Sustainable Improvements in Mechanical and Tribological Properties of AA2017-Aluminum Nitride Composites: A Comprehensive Investigation and Numerical Analysis," in *E3S Web of Conferences*, EDP Sciences, Jul. 2024. https://doi.org/10.1051/e3sconf/202455201035

[12] E. W. A. Fanani, E. Surojo, A. R. Prabowo, and H. I. Akbar, "Recent progress in hybrid aluminum composite: Manufacturing and application," *Metals (Basel).*, vol. 11, no. 12, Dec. 2021, https://doi.org/10.3390/met11121919

[13] A. B. Gurulakshmi, M. V. Rama Sundari, S. Lakhanpal, K. Dhamija, A. Parmar, and Q. Mohammad, "Steel Chips Reinforcement in Aluminum-Based Composites: Revolutionizing Manufacturing via Stir Casting Technique," in *E3S Web of Conferences*, EDP Sciences, Mar. 2024. https://doi.org/10.1051/e3sconf/202450701044

[14] N. A. TANIŞ *et al.*, "An Investigation of Production and Properties of RHA Reinforced Hybrid Composites by Vacuum Infiltration Method," *Uluslararası Muhendislik Arastirma ve Gelistirme Dergisi*, vol. 13, no. 2, pp. 704–710, Jun. 2021, https://doi.org/10.29137/umagd.913816

[15] S. Gopinath, M. Prince, and G. R. Raghav, "Enhancing the mechanical, wear and corrosion behaviour of stir casted aluminium 6061 hybrid composites through the incorporation of boron nitride and aluminium oxide particles," *Mater. Res. Express*, vol. 7, no. 1, 2020, https://doi.org/10.1088/2053-1591/ab6c1d

[16] M. R. Nasresfahani and M. Shamanian, "Characterization of Al1100-RHA composite developed by accumulative roll bonding," *J. Compos. Mater.*, vol. 53, no. 15, pp. 2047–2052, Jun. 2019, https://doi.org/10.1177/0021998318817938

[17] G. G. Holzschuh, D. S. Dörr, J. A. R. Moraes, and S. B. Garcia, "Metal matrix production: Casting of recycled aluminum cans and incorporation of rice husk ash and magnesium," *Journal of Composite Materials*, vol. 54, no. 22. SAGE Publications Ltd, pp. 3229–3241, Sep. 01, 2020. https://doi.org/10.1177/0021998320911964

[18] N. A. Latif *et al.*, "Crystalline rice husk silica reinforced AA7075 aluminium chips by cold compaction method," *Materwiss. Werksttech.*, vol. 52, no. 10, pp. 1121–1128, Oct. 2021, https://doi.org/10.1002/mawe.202000319

[19] N. F. Mohd Joharudin, N. A. Latif, M. S. Mustapa, N. A. Badarulzaman, and M. F. Mahmod, "Physical Properties and Hardness of Treated Amorphous Silica as Reinforcement of AA7075 Recycled Aluminum Chip," in *IOP Conference Series: Materials Science and Engineering*, Institute of Physics Publishing, Jun. 2020. https://doi.org/10.1088/1757-899X/824/1/012015

[20] H. Zuhailawati, M. N. Halmy, I. P. Almanar, and B. K. Dhindaw, "Friction stir processed of 6061-t6 aluminum alloy reinforced with silica from rice husk ash," in *Advanced Materials Research*, Trans Tech Publications Ltd, 2014, pp. 227–230. https://doi.org/10.4028/www.scientific.net/AMR.1024.227

[21] R. Ahmed, K. S. Prashanth, T. Annapurna, A. Jain, P. Maan, and I. Khan, "Revolutionizing Aluminum-Based Composite Manufacturing: Harnessing Fly Ash and Rice Husk Ash Reinforcement through Stir Casting for Sustainability," in *E3S Web of Conferences*, EDP Sciences, Mar. 2024. https://doi.org/10.1051/e3sconf/202450701048

[22] Md. R. Hossain, Md. H. Ali, Md. Al Amin, Md. G. Kibria, and Md. S. Ferdous, "Fabrication and Performance Test of Aluminium Alloy-Rice Husk Ash Hybrid Metal Matrix Composite as Industrial and Construction Material," *International Journal of Engineering Materials and Manufacture*, vol. 2, no. 4, pp. 94–102, Dec. 2017, https://doi.org/10.26776/ijemm.02.04.2017.03

[23] O. O. Joseph, J. O. Dirisu, J. Atiba, S. Ante, and J. A. Ajayi, "Mechanical, and corrosive properties of AA7075 aluminium reinforced with rice husk ash particulates," *Mater. Res. Express*, vol. 10, no. 11, Nov. 2023, https://doi.org/10.1088/2053-1591/ad0dd3

[24] A. Bahrami, M. I. Pech-Canul, C. A. Gutiérrez, and N. Soltani, "Microstructure and properties of bilayer-graded Al-matrix composites by one-step pressureless infiltration of B4C/rice-husk ash preforms," in *MRS Advances*, Materials Research Society, 2015, pp. 7–12. https://doi.org/10.1557/opl.2016.68

[25] O. P. Abolusoro, M. C. Khoathane, and W. Mhike, "Mechanical and microstructural characteristics of recycled aluminium matrix reinforced with rice husk ash," *AIMS Mater. Sci.*, vol. 11, no. 5, pp. 918–934, 2024, https://doi.org/10.3934/MATERSCI.2024044

[26] Z. Ahmad and S. Khan, "Mechanical characterization of LM25 alloy matrix composite reinforced with boron carbide," *Journal of Composite Materials*, vol. 55, no. 22. SAGE Publications Ltd, pp. 3151–3158, Sep. 01, 2021. https://doi.org/10.1177/00219983211005513

[27] A. H. Mohamed Ariff, O. Jun Lin, D. W. Jung, S. Mohd Tahir, and M. H. Sulaiman, "Rice Husk Ash as Pore Former and Reinforcement on the Porosity, Microstructure, and Tensile Strength of Aluminum MMC Fabricated via the Powder Metallurgy Method," *Crystals (Basel).*, vol. 12, no. 8, Aug. 2022, https://doi.org/10.3390/cryst12081100

[28] V. Gupta, B. Singh, and R. K. Mishra, "Microstructural and mechanical characterization of novel AA7075 composites reinforced with rice husk ash and carbonized eggshells," *Proceedings of the Institution of Mechanical Engineers, Part L: Journal of Materials: Design and Applications*, vol. 235, no. 12, pp. 2666–2680, Dec. 2021, https://doi.org/10.1177/14644207211031265

[29] A. Chinnamahammad Bhasha and K. Balamurugan, "Fabrication and property evaluation of Al 6061 + x% (RHA + TiC) hybrid metal matrix composite," *SN Appl. Sci.*, vol. 1, no. 9, Sep. 2019, https://doi.org/10.1007/s42452-019-1016-0

[30] T. Hasan, M. Wadud, M. H. Niaz, Md. K. Uddin, and M. S. Islam, "Fabrication and Characterization of Rice Husk Ash Reinforced Aluminium Matrix Composite," *Malaysian Journal on Composites Science and Manufacturing*, vol. 14, no. 1, pp. 34–43, Jul. 2024, https://doi.org/10.37934/mjcsm.14.1.3443

[31] M. Laad, V. S. Jatti, and S. Yadav, "Comparative Study between SiC Reinforced Al 64430 Metal Matrix Composites and RHA Reinforced Al 64430 Metal Matrix Composites," *Adv. Mat. Res.*, vol. 1119, pp. 234–238, Jul. 2015, https://doi.org/10.4028/www.scientific.net/amr.1119.234

[32] N. Srivast, L. K. Singh, and B. Kamesh, "Multiscale Modelling and Simulation of 3D Effective Homogenization for Material Properties of MWCNT and RHA Reinforced in Al P0507 Matrix Composite." Jun. 28, 2023. https://doi.org/10.21203/rs.3.rs-3102520/v1

[33] S. Saravanakumar, S. Gopalakrishnan, and K. Kalaiselvan, "Development of empirical relationships for prediction of mechanical and wear behavior of copper matrix surface composite by friction stir processing technique," *Archives of Metallurgy and Materials*, vol. 66, no. 2, pp. 617–626, 2021, https://doi.org/10.24425/amm.2021.135899

[34] Z. H. Li, H. Yan, Z. Hu, and X. C. Song, "Fluidity of ADC12 + xLa aluminum alloys," *Rare Metals*, vol. 40, no. 5, pp. 1191–1197, May 2021, https://doi.org/10.1007/s12598-014-0383-3

[35] H. S. Bang, H. I. Kwon, S. B. Chung, D. U. Kim, and M. S. Kim, "Experimental Investigation and Numerical Simulation of the Fluidity of A356 Aluminum Alloy," *Metals (Basel).*, vol. 12, no. 11, Nov. 2022, https://doi.org/10.3390/met12111986

[36] Zayad M. Sheggaf, Sharafaddeen S. Wanis Ehzazat, and Almabrouk A. Dhaw Esdeira, "Fluidity of Aluminum Piston Alloy with Different Amount of Pouring Temperature," *Bani Waleed University Journal of Humanities and Applied Sciences*, vol. 8, no. 3, pp. 31–36, Sep. 2023, https://doi.org/10.58916/jhas.v8i3.111

[37] I. Dinaharan, K. Kalaiselvan, and N. Murugan, "Influence of rice husk ash particles on microstructure and tensile behavior of AA6061 aluminum matrix composites produced using friction stir processing," *Composites Communications*, vol. 3, pp. 42–46, Mar. 2017, https://doi.org/10.1016/j.coco.2017.02.001

[38] Mohammed A. Abuqunaydah, Zayad M. Sheggaf, Muheieddin Meftah Elghanudi, and Salem A. Salem, "Recyclability of aluminium piston alloy," *Bani Waleed University Journal of Humanities and Applied Sciences*, vol. 8, no. 3, pp. 99–103, 2023, https://doi.org/10.58916/jhas.v8i3.122